



## IDENTIFICATION OF COSMOIIN AS A BIOACTIVE FLAVONOID IN *Memecylon randerianum* S.M. Almeida & M.R. Almeida: INSIGHTS INTO ITS ANTICANCER POTENTIAL

M.V. Lakshmi, and T.S. Swapna\*

Department of Botany, University of Kerala, Kariavattom, Thiruvananthapuram - 695 581, Kerala (India)  
\*e-mail: swapnats@yahoo.com

Received 2 June, 2025; accepted 8 February, 2026)

### ABSTRACT

The phytopharmaceutical industry increasingly employs advanced medicinal chemistry tools, including molecular docking, to facilitate the rational design and development of effective therapeutics against complex diseases such as cancer. In the present study, the anticancer potential of phytoconstituents from *Memecylon randerianum* was evaluated against Dalton's lymphoma ascites (DLA) and Ehrlich ascites carcinoma (EAC) tumour cell lines. The cytotoxic activity of the plant extract was further assessed using HeLa cervical cancer cells, MCF-7 breast cancer cells, and L929 fibroblast cell lines through the MTT assay. High-resolution liquid chromatography–mass spectrometry (HR-LCMS) analysis was performed to identify the chemical constituents present in the leaf extract. An *in silico* approach was subsequently employed to validate the pharmacological relevance and bioactivity of the identified compounds. Cosmoiin emerged as the predominant phytoconstituent in *M. randerianum* leaves. The ADMET characteristics of cosmoiin were predicted and analysed using the pkCSM and SwissADME tools. Protein-ligand interactions were visualised through two-dimensional diagrams generated using LigPlot+. The findings suggest that the cytotoxic effects exhibited by *M. randerianum* against cancer cell lines may be attributed to the presence of bioactive flavonoid, cosmoiin, highlighting its potential as a promising source for the development of novel anticancer drug leads.

**Keywords:** Bioactive compound; cosmoiin; drug lead, flavonoid, *in silico*, phytoconstituents

### INTRODUCTION

Cancer, with its diverse forms and associated complications, remains a major global health challenge due to alarmingly high incidence and mortality rates. In 2020 alone, approximately 19.3 million new cases and nearly 10 million deaths were reported worldwide (Cao *et al.*, 2021). To date, more than 277 types of cancer have been identified, among which breast cancer is the most prevalent, carrying high mortality among women (Arzmi *et al.*, 2023). No cancer treatment exists that has zero side effects. The scientific community has not so far been able to develop effective anti-cancer drugs with 100% safety. The rapid emergence of drug resistance has further complicated disease management, especially in cancer therapy, necessitating the exploration of alternative harmonizing treatment strategies (Raafat Hamed *et al.*, 2023; Sneka *et al.*, 2023). The increasing incidence of adverse effects associated with synthetic drugs has boosted research focus on medicinal plants as a safer and more effective therapeutic alternative. Presently, many plant species have gained great attention owing to their anticancer, antioxidant and anti-inflammatory properties (Guan and He, 2015). Numerous natural

products identified so far have been studied in various stages of clinical trials for cancer treatment. Generally, the plants demonstrating anticancer activity possess a variety of phyto-chemicals like phenols, alkaloids, flavonoids, etc. The therapeutic properties of unexplored plant species require systematic scientific validation to identify and develop effective drug leads. Several members of genus *Memecylon* are used in traditional medicine, with the most relevant species being *M. randerianum*.

*Memecylon* has both medicinal and horticultural values (Solaiman *et al.*, 2015). The information on the anticancer activity of *Memecylon* species is very scanty. *M. randerianum* (family Melastomataceae) is an indigenous medicinal shrub used both as a single and in junction with other medicinal plants to treat diabetes, jaundice or infectious hepatitis, skin disorders like herpes, chickenpox, and psoriasis (Hegde and Hungund, 2021). It is a woody shrub that grows up to 5-6 m tall, and its leaves are rich in secondary metabolites like flavonoids, glycosides, phenols, saponins, and tannins (Hegde and Hungund, 2021). The leaf decoction of *M. randerianum* has traditionally been used for the treatment of diarrhoea, bacterial infections, inflammatory conditions, and various skin disorders (Sivu *et al.*, 2013). However, this plant species remains underexplored from phytochemical and pharmacological perspectives. The present study was aimed to evaluate the anticancer potential of different parts of *M. randerianum* such as leaf, stem, and root, using various human cancer cell lines. High-resolution liquid chromatography–mass spectrometry quadrupole time-of-flight (HR-LCMS-QTOF) technique was used to identify the bioactive compounds present in its crude extracts. Furthermore, molecular docking analysis of the most abundant compound was performed against the selected cancer-related proteins. We have already reported the *in silico* properties of cosmosiin (Lakshmi and Swapna, 2021), however, its occurrence in *M. randerianum* and integrated evaluation of *in vitro* cytotoxic activity as well as *in silico* analysis have not so far been reported.

## MATERIALS AND METHODS

### *Cell lines, chemicals, and drugs*

The cell lines such as Dalton's lymphoma ascites (DLA), Ehrlich ascites carcinoma (EAC), human cervical carcinoma (HeLa), human breast adenocarcinoma (MCF-7), and murine fibroblast (L929), used in the present study were purchased from the National Centre for Cell Science (NCCS), Pune (India), and maintained in Dulbecco's modified Eagles medium (DMEM) [Sigma Aldrich, USA] supplemented with 10% fetal bovine serum (FBS), 100 U mL<sup>-1</sup> penicillin, and 100 µg mL<sup>-1</sup> streptomycin and kept at 37°C in an incubator with 5% CO<sub>2</sub>. All solvents, reagents, and analytical-grade chemical were purchased from Sigma-Aldrich (Steinheim, Germany) and Himedia (India). The reagents were prepared in a glass apparatus using distilled water with suitable solvents.

### *Collection, identification, and preparation of plant materials*

The different plant parts of *M. randerianum* (leaf, stem and root) were collected from the Campus of the University of Kerala, Thiruvananthapuram (India). The identification of plant material was authenticated by the curator in KUBH (Kerala University Botany Herbarium) and the sample specimen voucher was submitted to KUBH vide Voucher No. KUBH 6434. The leaves, stem, and roots of the plant were separately chopped into small pieces, shade-dried, and finely powdered by using an electric blender. The finely powdered samples were stored in air-tight containers at room temperature. The coarse powder was then subjected to continuous extraction with organic solvents of increasing polarity, such as petroleum ether, chloroform, acetone, methanol, and water, by the Soxhlet method for 6 h (Kausar *et al.* 2017). Then the extract was filtered using Whatman filter paper No. 1 and stored at 4°C. It is then used for further analysis.

### *Evaluation of anti-cancer activity*

The preliminary cytotoxic effect of different plant parts like leaf, stem and root was studied in Dalton's

lymphoma ascites (DLA) tumor cell lines and Ehrlich ascites carcinoma (EAC) cell lines. The cell viability was determined by trypan blue exclusion method (Talwar, 1984). In this method, the cell suspension was mixed with an equal volume of 0.4% trypan blue solution and incubated for 2-5 min at room temperature. A small amount of mixture was then loaded onto a hemocytometer and observed under a light microscope. The IC<sub>50</sub> value (half maximal inhibitory concentration) was determined from dose-response curves generated using different concentrations of plant extract. The percent inhibition values were plotted against the logarithm of extract concentrations to generate a dose-response curve. The experiments were performed in triplicate (n = 3) and percent cytotoxicity calculated using the following formula:

$$\text{Percentage of cytotoxicity} = \frac{\text{Number of Dead cells}}{\text{Number of Live cells} + \text{Number of Dead cells}} \times 100$$

Based on the preliminary cytotoxicity screening, the extract that showed the highest percentage was selected for *in vitro* anticancer effect against HeLa cervical cell line, MCF-7 cell lines, and L929 fibroblast cell lines by MTT assay (Mosmann, 1983). Approximately 1 x 10<sup>5</sup> cells mL<sup>-1</sup> were seeded in a 24 well plate, with complete growth medium (DMEM) and allowed to attach and grow. At ~80% confluence, the medium was replaced with fresh medium containing different concentrations of leaf extract (6.25-100 µg mL<sup>-1</sup>). The cells were incubated for 48 h, and the medium was replaced with fresh medium. Then 20 µL of 0.5% 3-(4,5-dimethylthiazol-2-yl)-2,5-diphenyltetrazolium bromide (MTT) was added to each well and incubated for 4 h. The formazan crystals formed were dissolved in dimethyl sulfoxide, and the absorbance was measured at 570 nm in UV-vis spectrophotometer (Systronics, India). The percentage viability was calculated using the formula:

$$\text{Percentage Cell death} = \frac{\text{Ab of control} - \text{Ab of sample}}{\text{Ab of control}} * 100$$

The viable cells excluded the dye and appeared transparent, whereas non-viable cells took up the dye and appeared blue. The number of stained and unstained cells was counted, and the percentage of viable cells calculated based on the proportion of unstained cells to the total number of cells. The IC<sub>50</sub> value (half maximal inhibitory concentration) was determined from dose-response curves generated using different concentrations of plant extract. The percent inhibition values were plotted against the logarithm of extract concentrations to generate a dose-response curve. The experiments were performed in triplicate.

#### ***HR-LCMS-QTOF analysis***

To detect the chemical components, present in leaf extract, high-resolution liquid chromatography-mass spectrometry/mass spectrometry-quadrupole time-of-flight (HR-LCMS-QTOF) analysis was performed at the Sophisticated Analytical Instrument Facility (SAIF), Indian Institute of Technology (IIT), Pawai, Mumbai. It was performed using Agilent high resolution liquid chromatography and mass spectrometry (model-G6550A, equipped with a dual AJS ESI ion source) with 0.01% mass resolution. Chromatographic separation was done using a ZORBAX Eclipse Plus C18 column (2.1 mm × 100 mm, 1.8 µm). The column temperature was maintained at 35°C. The mobile phase consisted of solvent A (0.1% formic acid in water) and solvent B (0.1% formic acid in acetonitrile). Elution was carried out at a flow rate of 0.3 mL min<sup>-1</sup> using a gradient program ranging from 5 to 95% solvent B over 30 min. The injection volume was set at 5 µL.

#### ***Docking studies***

Molecular docking of the most abundant compound, identified during HR-LCMS-QTOF analysis, was done to find out the best-fit orientation of the ligand and target protein. Since many reports showed that matrix metalloproteinase (MMPs), tyrosine kinase domain 1 (TKIs) and vascular endothelial growth factor receptor (VEGFR) are potential biomarkers serving as vital mediators of signal transduction and cancer cell proliferation, angiogenesis, and apoptosis (Mondal *et al*, 2020; Mongre *et al*, 2021; Elrazaz *et al*, 2021), TK1 (1T46), VEGFR-2 (3VHE), and MMP-9 (1GKC)

were selected as target proteins. These target proteins were docked with the selected ligands such as cosmosiin, apigenin, cinnamic acid, ursolic acid, rutin, isorhamnetin, gallic acid, quercetin, catechin using AutoDock vina. ADMET properties of the compound were calculated and analysed through pkCSM tool and SwissADME. The structure of the target protein interacting with the best conformation of ligand in pdb format was generated using Pymol.

#### **Ligand preparation and selection of target proteins**

The structure of the ligand was available in Pubchem (<https://pubchem.ncbi.nlm.nih.gov/>). The canonical SMILES notation of ligand was taken from Pubchem database at NCBI (<https://www.ncbi.nlm.nih.gov/>), and 3D structure in pdb format was obtained using the tool CORINA (COoRdINAtes, <https://mn-am.com/products/corina/>). The prediction of active site residues of target protein was made using tools like Castp and PDBSum (<http://sts.bioe.uic.edu/castp/index.html?2cpk>, <https://www.ebi.ac.uk/thornton-srv/software/PDBsum1/>). The Discovery Studio visualizer was also used for the analysis of protein structure and bond interactions between the ligand and active residues of the target protein.

#### **AutoDock analysis**

The protein and ligand were prepared and saved in .pdbqt format. Grid parameters were set based on the position of active site residues. The input file for docking was saved in a text file config.txt, which includes receptor and ligand files in pdbqt format and grid parameters. The 2D diagrammatic representation of interaction (both bonded and non-bonded interactions) between the attached ligand and protein was done using LigPlot+ tool (Laskowski and Swindells, 2011). The ADMET properties of cosmosiin were assessed and analysed through pkCSM tool and Swiss ADME.

#### **Statistical analysis**

All the biological experiments were conducted in triplicate in a completely randomized design and the results were expressed as mean  $\pm$  standard error. The data were analysed using one-way and two-way ANOVA, followed by Duncan's multiple range test (Iazzetti *et al.*, 2000). The significance of F value was set at  $p < 0.05$ .

## **RESULTS AND DISCUSSION**

In the present investigation, the *in vitro* cytotoxic potential of methanolic extracts, prepared from leaf, stem, and roots of *M. randerianum*, was evaluated against Dalton's lymphoma ascites (DLA) and Ehrlich ascites carcinoma (EAC) cell lines using trypan blue exclusion assay. This assay distinguishes viable cells, which maintain membrane integrity and exclude the dye, from non-viable cells that absorb the dye due to compromised membranes. The results demonstrated a clear dose-dependent cytotoxic effect of *M. randerianum* extracts against both DLA and EAC cell lines. Among the highest cytotoxicity against the test samples, the leaf extract exhibited DLA cells, with a maximum

**Table 1: *In vitro* cytotoxic effect of different parts of *M. randerianum* against DLA cell lines**

| Concentration<br>( $\mu\text{g mL}^{-1}$ ) | Cell death (%) |                 |                 | Normal cell line<br>(rat spleen cells) |
|--|----------------|-----------------|-----------------|--|
|  | Leaf           | Stem            | Root            |  |
| 10   | 18 $\pm$ 2.3   | 2.69 $\pm$ 0.03 | 2.8 $\pm$ 0     | 0 $\pm$ 0.00                           |
| 20   | 27 $\pm$ 2.1   | 3.67 $\pm$ 0.04 | 2.91 $\pm$ 0.01 | 0 $\pm$ 0.00                           |
| 50   | 39 $\pm$ 1.6   | 5.65 $\pm$ 0.46 | 3.11 $\pm$ 0.04 | 0 $\pm$ 0.00                           |
| 100  | 56 $\pm$ 1.8   | 11 $\pm$ 0.29   | 3.9 $\pm$ 0.4   | 0 $\pm$ 0.00                           |
| 200  | 90 $\pm$ 1.9   | 15.4 $\pm$ 0.62 | 5.5 $\pm$ 0.7   | 4 $\pm$ 0.00                           |
| IC <sub>50</sub> value                     | 100.86         | 591.01          | 1529.05         | 2468.55                                |

cell death of 90  $\pm$  1.9% observed at a concentration of 200  $\mu\text{g mL}^{-1}$  (Table 1). Stem and root extracts also showed increasing cytotoxicity with rising concentrations, with maximum activity recorded at the highest tested dose. A similar dose-dependent cytotoxic pattern was observed against EAC cell lines, wherein all three extracts

**Table 2: *In vitro* cytotoxic effect of different parts of *M. randerianum* against EAC cell lines**

| Concentration<br>( $\mu\text{g mL}^{-1}$ ) | Cell death (%) |                 |                 |  |
|--|----------------|-----------------|-----------------|--|
|  | Leaf           | Stem            | Root            | Normal cell line<br>(rat spleen cells) |
| 10   | 17 $\pm$ 2.6   | 3.77 $\pm$ 0.01 | 3.70 $\pm$ 0.00 | 0 $\pm$ 0.00                           |
| 20   | 29 $\pm$ 2.5   | 4.02 $\pm$ 0.14 | 3.83 $\pm$ 0.01 | 0 $\pm$ 0.00                           |
| 50   | 36 $\pm$ 2.7   | 5.11 $\pm$ 0.44 | 3.89 $\pm$ 0.04 | 0 $\pm$ 0.00                           |
| 100  | 55 $\pm$ 2.0   | 5.65 $\pm$ 1.36 | 4.30 $\pm$ 0.6  | 0 $\pm$ 0.00                           |
| 200  | 86 $\pm$ 2.6   | 8.89 $\pm$ 2.41 | 7.50 $\pm$ 0.9  | 4 $\pm$ 0.00                           |
| IC <sub>50</sub> value                     | 104.95         | 980.39          | 1184.83         | 2468.55                                |

**Table 3: Percentage cell viability by the methanolic leaf extract of *M. randerianum* against L929 fibroblast and HeLa (cervical carcinoma) cell lines**

| Concentration<br>( $\mu\text{g mL}^{-1}$ ) | Cell viability (%) |                 |
|--|--------------------|-----------------|
|  | L929 cell lines    | HeLa cell lines |
| Control                                    | 100.00             | 100.00          |
| 6.25                                       | 92.43              | 91.64           |
| 12.50                                      | 89.84              | 90.89           |
| 25   | 84.22              | 86.38           |
| 50   | 76.53              | 73.66           |
| 100  | 73.73              | 66.79           |
| IC <sub>50</sub> values                    | 208.25             | 152.27          |

**Table 4: Percentage cell inhibition by the methanolic leaf extract of *M. randerianum* against MCF-7 cell lines**

| Concentration<br>( $\mu\text{g mL}^{-1}$ ) | Percent inhibition<br>in MCF-7 cell line |
|--|--|
| Cell control                               | 0  |
| Vehicle control                            | 98.66                                    |
| 25   | 59.53                                    |
| 50   | 51.73                                    |
| 100  | 49.13                                    |
| 200  | 34.68                                    |
| 400  | 36.71                                    |
| 800  | 36.42                                    |
| IC <sub>50</sub> values                    | 167.35                                   |

LC-MS/QTOF analysis was performed, leading to the identification of several major phyto-constituents (Table 6; Fig. 2). Notably, many of the identified compounds belong to the class of polyphenolic metabolites, particularly flavonoids and tannins, which are well known for their diverse pharmacological properties. These compounds have been widely reported to exhibit significant antiproliferative and pro-apoptotic activities against various cancer cells, thereby contributing to the anticancer potential of plant-derived extracts. The methanolic leaf extract exhibited IC<sub>50</sub> values of 100.86  $\mu\text{g mL}^{-1}$  against DLA cells and 104.95  $\mu\text{g mL}^{-1}$  against EAC cells (Table 5). In contrast, a much higher IC<sub>50</sub> value was observed in normal spleen cells (2468.55  $\mu\text{g mL}^{-1}$ ), indicating comparatively lower toxicity toward normal cells. The IC<sub>50</sub> values for L929, HeLa, and

exhibited pronounced toxicity, particularly at 200  $\mu\text{g mL}^{-1}$  (Table 2). These findings suggest that *M. randerianum*, especially its leaf extract, has significant anticancer activity against ascites tumour models.

Further evaluation using MTT assay revealed cytotoxic effects of methanolic leaf extract on L929 murine fibroblast and HeLa human

cervical cancer cell lines (Table 3). Treated cells exhibited marked morphological alterations, including a transition from normal spindle-shaped morphology to star-shaped, shrunken, and damaged forms, indicative of cytotoxicity and apoptosis (Fig. 1 & 2). Cell proliferation showed significant inhibition in a concentration-dependent manner, with a decrease in cell viability observed at higher extract concentrations. These morphological and viability changes are characteristic features associated with programmed cell death.

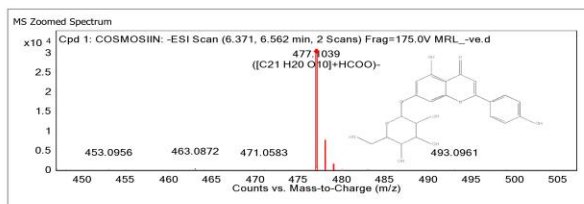
The methanolic leaf extract exhibited IC<sub>50</sub> values of 100.86  $\mu\text{g mL}^{-1}$  against DLA cells and 104.95  $\mu\text{g mL}^{-1}$  against EAC cells (Table 5). In contrast, a much higher IC<sub>50</sub> value was observed in normal spleen cells (2468.55  $\mu\text{g mL}^{-1}$ ), indicating comparatively lower toxicity toward normal cells. The IC<sub>50</sub> values for L929, HeLa, and MCF-7 cell lines were 208.25, 152.27, and 167.35  $\mu\text{g mL}^{-1}$ , respectively (Table 4), whereas the standard drug 5-fluorouracil showed an IC<sub>50</sub> of 86.49  $\mu\text{g mL}^{-1}$ . These results highlight the moderate to strong anticancer efficacy of *M. randerianum* extracts with a degree of selectivity toward cancer cells.

The observed cytotoxic activity may be attributed to the presence of bioactive secondary metabolites such as alkaloids, flavonoids, phenolics, terpenoids, and saponins, which are well-documented for their anticancer properties (Usman *et al.*, 2022). To further elucidate the molecular basis of the observed biological activity, high-resolution

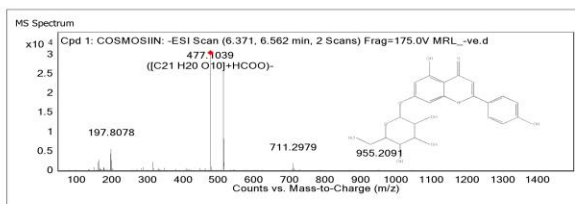
**Table 5: IC<sub>50</sub> values for the methanolic leaf extract against different cancer cell lines**

| Cell lines  | IC <sub>50</sub> value (µg mL <sup>-1</sup> ) |
|---|---|
| Dalton's lymphoma ascites (DLA) tumour cell lines | 100.86  |
| Ehrlich's ascites carcinoma (EAC) cell lines      | 104.95  |
| Normal spleen cells                               | 2468.55                                       |
| Murine fibroblast (L929) cell lines               | 208.25  |
| Henrietta Lacks (HeLa) cell lines                 | 152.27  |
| Michigan cancer foundation-7 (MCF-7) cell lines   | 167.35  |
| 5-Fluorouracil                                    | 86.49   |

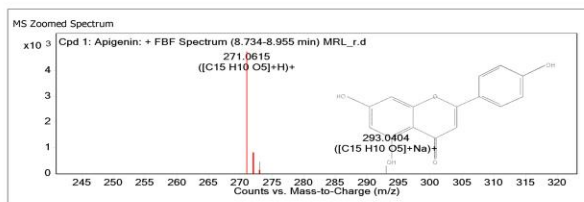
MCF-7 cell lines were 208.25, 152.27, and 167.35 µg mL<sup>-1</sup>, respectively (Table 4), whereas the standard drug 5-fluorouracil showed an IC<sub>50</sub> of 86.49 µg mL<sup>-1</sup>. These results highlight the moderate to strong anticancer efficacy of *M. randerianum* extracts with a degree of selectivity toward cancer cells.



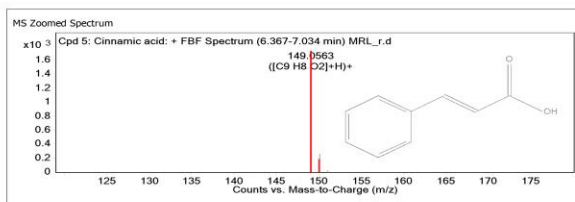
MS Spectrum of Cosmosin



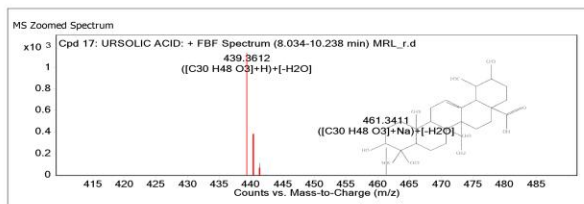
MS Spectrum of Cosmosin



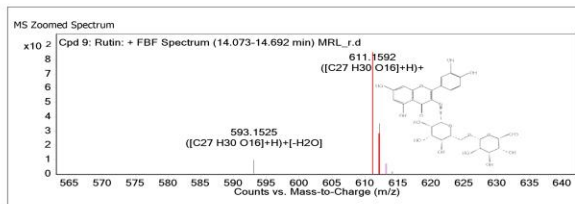
MS Spectrum of Apigenin



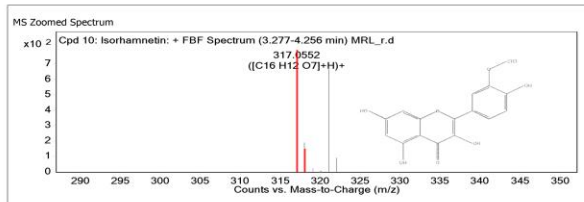
MS Spectrum of Cinnamic acid



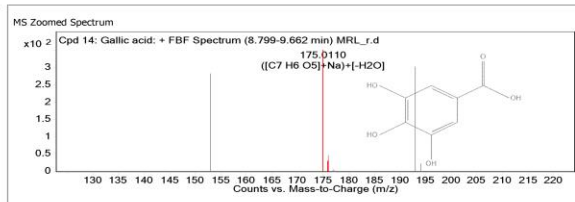
MS Spectrum of Ursolic acid



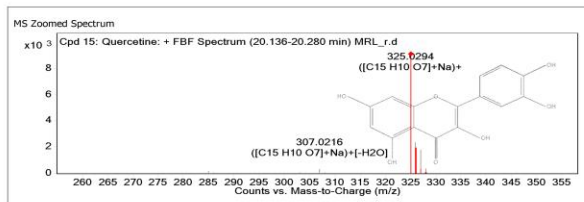
MS Spectrum of Rutin



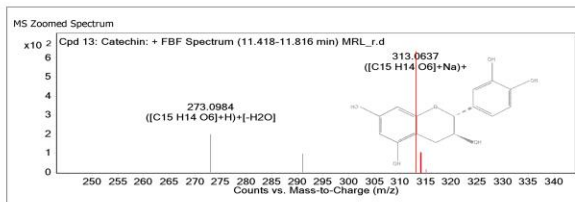
MS Spectrum of Isorhamnetin



MS Spectrum of Gallic acid



MS Spectrum of Quercetin



MS Spectrum of Catechin

**Fig. 1: MS spectrum and structure of the compounds found in the methanolic leaf extract of *Memecylon randerianum***

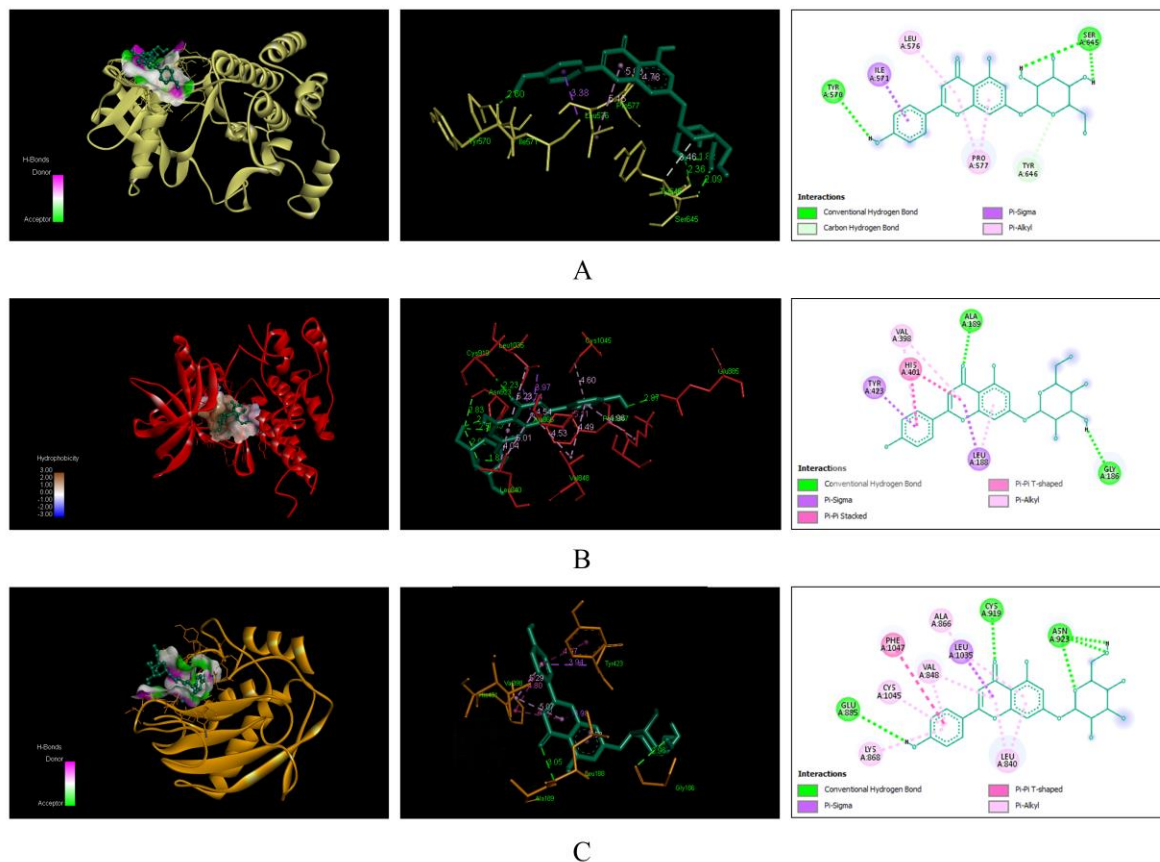


**Fig. 2: Molecular interaction of cosmosiin with the targeted receptor proteins (A) TK1, (B) VEGFR-2, and (C) MMP-9**

**Table 6: Bioactive compounds detected in the methanolic leaf extract of *M. randerianum***

| Name of the compounds | Retention time (min) | Abundance (intensity, counts sec <sup>-1</sup> ) | Mass (m/z) | Chemical formula                                | Double bond equivalent (ppm) |
|-----------------------|----------------------|--|------------|---|------------------------------|
| Cosmosiin             | 6.485                | 6255.17  | 432.1056   | C <sub>21</sub> H <sub>20</sub> O <sub>10</sub> | 0.12                         |
| Apigenin              | 8.799                | 4744   | 270.0544   | C <sub>15</sub> H <sub>10</sub> O <sub>5</sub>  | -5.69                        |
| Cinnamic acid         | 6.678                | 1735   | 148.0485   | C <sub>9</sub> H <sub>8</sub> O <sub>2</sub>    | 26.65                        |
| Ursolic acid          | 9.434                | 1131   | 456.3642   | C <sub>30</sub> H <sub>48</sub> O <sub>3</sub>  | -8.40                        |
| Rutin                 | 14.241               | 851  | 610.1523   | C <sub>27</sub> H <sub>30</sub> O <sub>16</sub> | 1.82                         |
| Isorhamnetin          | 4.116                | 663  | 316.048    | C <sub>16</sub> H <sub>12</sub> O <sub>7</sub>  | 32.45                        |
| Gallic acid           | 8.799                | 303  | 170.0322   | C <sub>7</sub> H <sub>6</sub> O <sub>5</sub>    | -62.61                       |
| Quercetin             | 20.136               | 265  | 302.0385   | C <sub>15</sub> H <sub>10</sub> O <sub>7</sub>  | 13.73                        |
| Catechin              | 11.536               | 97   | 290.0752   | C <sub>15</sub> H <sub>14</sub> O <sub>6</sub>  | 13.31                        |

The observed cytotoxic activity may be attributed to the presence of bioactive secondary metabolites such as alkaloids, flavonoids, phenolics, terpenoids, and saponins, which are well-documented for their anticancer properties (Usman et al., 2022). To further elucidate the molecular basis of the observed biological activity, high-resolution LC-MS/QTOF analysis was performed, leading to the identification of several major phytoconstituents (Table 6; Fig. 2). Among these, polyphenolic compounds, particularly flavonoids and tannins, have been widely reported to exhibit anti-proliferative and pro-apoptotic effects in cancer cells.

Molecular docking studies provided additional mechanistic insights into the anticancer potential of the identified compound cosmosiin (Table 7; Fig. 5). The *in silico* pharmacological properties of

**Table 7: The Binding energy of the three receptor proteins**

| Receptor proteins                           | Binding energy<br>(kcal mol <sup>-1</sup> ) |
|---|---|
| Tyrosine kinase domain 1 (1T46)             | -6.6  |
| Vascular endothelial growth factor-2 (3VHE) | -11.2                                       |
| Matrix metalloproteinase-9 (1GKC)           | -8.5  |

cosmosiin have been reported earlier (Lakshmi and Swapna, 2021). Cosmosiin exhibited strong binding affinities with selected cancer-related target proteins, with binding energies,

exceeding -6.5 kcal mol<sup>-1</sup>. Notably the interaction with vascular endothelial growth factor receptor-2 (VEGFR-2; PDB ID: 3VHE) showed the highest binding affinity (-11.20 kcal mol<sup>-1</sup>), while the tyrosine kinase domain (TK1; PDB ID: 1T46) exhibited the lowest binding energy (-6.6 kcal mol<sup>-1</sup>). These interactions suggest the potential of cosmosiin to interfere with angiogenesis and tyrosine kinase-mediated signalling pathways involved in tumour progression. Earlier studies have demonstrated the critical role of thymidylate synthase and tyrosine kinase inhibitors in cancer therapy by inducing apoptosis and inhibiting tumour growth (Hartmann *et al.*, 2009; Von Bubnoff *et al.*, 2009; Alam *et al.*, 2021). Additionally, inhibition of VEGFR-2-mediated angiogenesis has been recognized as an effective strategy for suppressing tumour development and metastasis (Saraswati *et al.*, 2013). The strong binding interactions observed in the present study are consistent with these reports and support the anticancer relevance of identified phytochemicals. The findings of this study demonstrate that *M. randerianum* contains bioactive compounds with significant *in vitro* anticancer potential, supported by cytotoxic assays and molecular docking analysis. These results suggest that *M. randerianum* represents a promising candidate for further pharmacological studies aimed at the development of plant-based anticancer therapeutics.

**Conclusion:** The present study established the promising anticancer potential of *Memecylon randerianum*, which may be attributed to its diverse phytochemical composition. The methanolic extracts prepared from the leaf, stem, and root of *M. randerianum* revealed the presence of several bioactive secondary metabolites with cytotoxic and antioxidant properties. Among the test extracts, the methanolic leaf extract showed comparatively higher cytotoxic activity against selected cancer cell lines, indicating the leaf as a rich source of bioactive compounds. HR-LCMS-QTOF analysis identified several phytoconstituents such as cosmosiin, apigenin, cinnamic acid, ursolic acid, rutin, isorhamnetin, gallic acid, quercetin, and catechin. Molecular docking revealed favourable interactions of these compounds with cancer-related target proteins. These findings highlight the pharmacological significance of *M. randerianum* and its potential in future anticancer drug discovery.

**Acknowledgements:** Authors are greatly thankful to the Council of Scientific and Industrial Research, New Delhi for providing the financial support to the present work, and to IIT Mumbai for their help in HR-LCMS-QTOF analysis.

**Conflict of interest:** Authors declare that they have no conflict of interest between them.

## REFERENCES

- Alam, M.M., Malebari, A.M., Syed, N., Neamatallah, T., Almalki, A.S., Elhenawy, A.A., *et al.*, 2021. Design, synthesis and molecular docking studies of thymol based 1,2,3-triazole hybrids as thymidylate synthase inhibitors and apoptosis inducers against breast cancer cells. *Bioorganic & Medicinal Chemistry*, **38**: 116136. [<https://doi.org/10.1016/j.bmc.2021.116136>].
- Arzmi, M.H., Anwar, P.P., Rabiou, M.M., Azraai, M., Razman, M., Hong-Seng, G., *et al.*, 2023. *Deep Learning in Cancer Diagnostics: A Feature-based Transfer Learning Evaluation*. Springer Nature, Singapore.
- Cao, W., Chen, H.D., Yu, Y.W., Li, N. and Chen, W.Q. 2021. Changing profiles of cancer burden worldwide and in China: A secondary analysis of the Global Cancer Statistics 2020. *Chinese Medical Journal*, **134**: 783-791.

- Elrazaz, E.Z., Serya, R.A., Ismail, N.S., Albohy, A., Abou El Ella, D.A. and Abouzid, K.A. 2021. Discovery of potent thieno [2, 3-d] pyrimidine VEGFR-2 inhibitors: Design, synthesis and enzyme inhibitory evaluation supported by molecular dynamics simulations. *Bioorganic Chemistry*, **113**: 105019. [<https://doi.org/10.1016/j.bioorg.2021.105019>].
- Guan, Y.S. and He, Q. 2015. Plant consumption and liver health. *Evidence-Based Complementary and Alternative Medicine*. **2015**: 824185. [<https://doi.org/10.1155/2015/824185>].
- Hartmann, J.T., Haap, M., Kopp, H.G. and Lipp, H.P. 2009. Tyrosine kinase inhibitors - A review on pharmacology, metabolism and side effects. *Current Drug Metabolism*, **10**: 470-481.
- Hegde, N.P. and Hungund, B.S. 2021. Isolation, identification and *in vitro* biological evaluation of phytochemicals from *Memecylon randerianum*: A medicinal plant endemic to Western Ghats of India. *Natural Product Research*, **35**: 5334-5338.
- Iazzetti, G., Burgess, J., Gardiner, D. and Ripps, A. 2000. Color stability of fluoride-containing restorative materials. *Operative Dentistry*, **25**: 520-525.
- Kausar, H., Abidin, L. and Mujeeb, M. 2017. Comparative assessment of extraction methods and quantitative estimation of thymoquinone in the seeds of *Nigella sativa* L. by HPLC. *International Journal of Pharmacognosy and Phytochemical Research*, **9**: 1425-1428.
- Lakshmi, M.V. and Swapna, T.S. 2021. A computational study on cosmosiin, an antiviral compound from *Memecylon randerianum*. *Medicinal Plants - International Journal of Phytomedicines and Related Industries*, **13**: 515-523.
- Laskowski, R.A. and Swindells, M.B. 2011. LigPlot+: Multiple ligand-protein interaction diagrams for drug discovery. *Journal of Chemical Information and Modeling*, **51**: 2778-2786.
- Mondal, S., Adhikari, N., Banerjee, S., Amin, S.A. and Jha, T. 2020. Matrix metalloproteinase-9 (MMP-9) and its inhibitors in cancer: A minireview. *European Journal of Medicinal Chemistry*, **194**: p.112260. [<https://doi.org/10.1016/j.ejmech.2020.112260>].
- Mongre, R.K., Mishra, C.B., Shukla, A.K., Prakash, A., Jung, S., Ashraf-Uz-Zaman, M., *et al.*, 2021. Emerging importance of tyrosine kinase inhibitors against cancer: Quo vadis to cure? *International Journal of Molecular Sciences*, **22**(21): 11659. [<https://doi.org/10.3390/ijms222111659>].
- Mosmann, T. 1983. Rapid colorimetric assay for cellular growth and survival: Application to proliferation and cytotoxicity assays. *Journal of Immunological Methods*, **65**: 55-63.
- Raafat Hamed, R.M., Dwedar, F., Bassyouni, R., Emira, A.S., El-Hmid, A. and Dowidar, M.A., *et al.*, 2023. Alarming antibiotic resistance pattern of bacterial isolates in neonatal sepsis: A study from Egypt. *Egyptian Journal of Medical Microbiology*, **32**: 1-10.
- Saraswati, S., Kanaujia, P.K., Kumar, S., Kumar, R. and Alhaider, A.A. 2013. Tylophorine exerts antiangiogenic and antitumor activity by targeting VEGFR-2-mediated angiogenesis. *Molecular Cancer*, **12**: 82. [<https://doi.org/10.1186/1476-4598-12-82>].
- Sivu, A.R., Pradeep, N.S., Rameshkumar, K.B. and Pandurangan, A.G. 2013. Evaluation of phytochemical, antioxidant and antimicrobial activities of *Memecylon* L. species from Western Ghats. *Indian Journal of Natural Products and Resources*, **4**: 363-370.
- Sneka, P., Mahalakshmi Krishnan, D., Hamsadwani, K. and Janakiraman, R. 2023. Changing pattern of drug resistance in *Candida*: A review. *Journal of Pharmaceutical Negative Results*, **14**: 1877-1880.
- Solaiman, A., Nishizawa, T., Sultana, N., Sarker, B., Rahman, R., Shahjahan, M., *et al.*, 2015. Antimicrobial and antioxidant activity analysis of some medicinal plants of Bangladesh. *Advances in Plants and Agriculture Research*, **2**: 00057. [<https://doi.org/10.15406/apar.2015.02.00057>].
- Talwar, G. 1984. *Handbook of Practical Immunology*. Vikas Publishing House, New Delhi, India.
- Usman, M., Khan, W.R., Yousaf, N., Akram, S., Murtaza, G., Kudus, K.A., *et al.*, 2022. Exploring the phytochemicals and anticancer potential of the members of Fabaceae family: A comprehensive review. *Molecules*, **27**(12): 3863. [<https://doi.org/10.3390/molecules27123863>].